Principles of leaky-mode photonic lattices: band flips and Bloch mode dynamics

Magnusson, Robert, Lee, Sun-Goo, Lee, Kyu, Hemmati, Hafez, Carney, Daniel, et al.

Robert Magnusson, Sun-Goo Lee, Kyu J. Lee, Hafez Hemmati, Daniel J. Carney, Pawarat Bootpakdeetam, Yeong Hwan Ko, "Principles of leaky-mode photonic lattices: band flips and Bloch mode dynamics," Proc. SPIE 10921, Integrated Optics: Devices, Materials, and Technologies XXIII, 109211E (4 March 2019); doi: 10.1117/12.2508984

SPIE.

Event: SPIE OPTO, 2019, San Francisco, California, United States

Invited Paper

Principles of leaky-mode photonic lattices: Band flips and Bloch mode dynamics

Robert Magnusson, Sun-Goo Lee, Kyu J. Lee, Hafez Hemmati, Daniel J. Carney,
Pawarat Bootpakdeetam, and Yeong Hwan Ko
Department of Electrical Engineering, University of Texas Arlington, Arlington, Texas 76019, USA

ABSTRACT

We present principles of leaky-mode photonic lattices explaining key properties enabling potential device applications. The one-dimensional grating-type canonical model is rich in properties and conceptually transparent encompassing all essential attributes applicable to two-dimensional metasurfaces and periodic photonic slabs. We address the operative physical mechanisms grounded in lateral leaky Bloch mode resonance emphasizing the significant influence imparted by the periodicity and the waveguide characteristics of the lattice. The effects discussed are not explainable in terms of local Fabry-Perot or Mie resonances. In particular, herein, we summarize the band dynamics of the leaky stopband revealing principal Bragg diffraction processes responsible for band-gap size and band closure conditions. We review Bloch wave vector control of spectral characteristics in terms of distinct evanescent diffraction channels driving designated Bloch modes in the lattice.

Keywords: guided-mode resonance effect, leaky-mode resonance, resonant waveguide gratings, metamaterials, Bloch modes, wave propagation in periodic media, leaky-band dynamics

1. INTRODUCTION

A photonic lattice is a periodic assembly of arbitrarily shaped particles. These particles can be made of metals, dielectrics, and semiconductors or their hybrid compositions. The lattice is, in general, three-dimensional (3D) with important variants in the form of 2D or 1D patterned films. The lattice operates in fundamental ways on incident light with ability to control and manipulate amplitude, phase, spectral distribution, polarization state, and local mode structure. Thus, nano- and microstructured films with subwavelength periodicity represent fundamental building blocks for a host of device concepts. For many real-world applications, attractive features of this device class include compactness, minimal interface count, high efficiency, potential monolithic fabrication, and attendant survivability under harsh conditions. The fundamental operational modality is available across the spectrum, from visible wavelengths to the microwave domain, by simple scaling of wavelength to period and pertinent materials selection.

Here, we address the physical basis behind the resonance effects inherent in the fundamental lattice, discuss the observed behavior, and mention example applications. The guided-mode resonance (GMR) concept refers to quasi-guided waveguide modes induced in periodic layers [1-24]. Whereas the canonical physical properties of the resonance are fully embodied in a one-dimensional (1D) lattice, the final device constructs are often patterned in a two-dimensional (2D) slab or film in which case we commonly refer to them as photonic crystal slabs or metasurfaces. These surfaces are capable of supporting lateral modes and localized field signatures with propagative and evanescent diffraction channels critically controlling the response. Local Fabry-Perot and Mie mode signatures are observable via computations within the structural geometry. It can be convincingly argued that local modes have no causal effects with lateral Bloch modes generating all key effects [25]. The subwavelength restriction of periodicity is usually maintained for efficient devices; however, it is also possible to generate interesting spectral behavior when this is not satisfied leading to unexpected device concepts [26]. The dominant second, or leaky, stopband exhibits many remarkable physical properties including band-edge transitions and bound states in the continuum. The Fourier harmonic content of the spatial modulation is key to understanding the band dynamics of these lattices. Multi-resonance effects are observed when Bloch eigenmodes are excited with more than one evanescent diffraction channels with the resulting spectral response clearly understood by invoking this process. We have shown how materially sparse leaky-mode photonic lattices may be nearly completely invisible to one polarization state while being opaque to the orthogonal polarization state with this property existing over significantly wide spectral bands [24]. Device concepts with experimental prototypes verifying theoretical predictions

*magnusson@uta.edu; phone 1 817 272-2672; fax 1 817 272-2253; www.leakymoderesonance.com

Integrated Optics: Devices, Materials, and Technologies XXIII, edited by Sonia M. García-Blanco, Pavel Cheben,
Proc. of SPIE Vol. 10921, 109211E · © 2019 SPIE · CCC code: 0277-786X/19/$18 · doi: 10.1117/12.2508984

include wideband reflectors [25], nonfocusing spatial filters [26], ultra-sparse reflectors and polarizers [24], single-layer bandpass filters [27], and multiparametric resonant sensors [28] were demonstrated by our group in the past.

In this paper, we discuss physical principles of resonant leaky-mode lattices. We present the band structure of the operational leaky stop band including the principles dominating the band dynamics such as band-gap width and band closure. Analytical and numerical results on the formation of the leaky stop band demonstrate that Bragg processes generated by spatial Fourier harmonics control the band transition dynamics. We discuss Bloch wave-vector spectral control and its use to implement doubly-resonant bandpass filters as well as angular robustness in guided-mode resonance spectra. The doubly-resonant bandpass-filter process, implemented by interference between high-Q and low-Q Bloch modes, has of late come to be marked as being analogous to electromagnetically-induced transparency (EIT).

2. THE BAND STRUCTURE OF THE LEAKY-MODE LATTICE

Nanopatterned surfaces and films with subwavelength periodicity sustain striking resonance effects as input light couples to leaky Bloch-type waveguide modes [11, 29]. In 1990, we coined the term "guided-mode resonance (GMR)" to clearly communicate the fundamental physics governing these phenomena [30]. Prior to that, in the earlier literature on the subject, authors often referred to these effects as being "anomalous." In recent years, traditional GMR resonance devices are often called metasurfaces or metamaterials [31-33]. We emphasize that these devices can have 1D or 2D lateral spatial modulation, or periodicity, as the resonance physics is not dependent on the type of periodicity in any fundamental ways. The resonance effects of interest here are observed in a slab, or film, geometry as the structure must be capable of supporting quasi-guided modes propagating laterally in the periodic lattice and hence being Bloch modes in common terminology. In the past, in the community of diffractive optics that preceded the metamaterials generation, such elements were sometimes called "waveguide gratings," a clear and physically-expressive descriptor. It has been well-known for a long time, on account of inherent design flexibility, that a plethora of differing spectral expressions is available with this device class thus providing a facile applications platform. Wide parametric design spaces allow control of light amplitude, phase, polarization, near-field intensity, light distribution, etc., on surfaces and within device volumes. 3D variants of this device class are possible in which waveguide gratings are interspersed with homogeneous films forming an operational stack. The second leaky stop band plays crucial roles in device operation; hence we summarize key points on the band structure here.

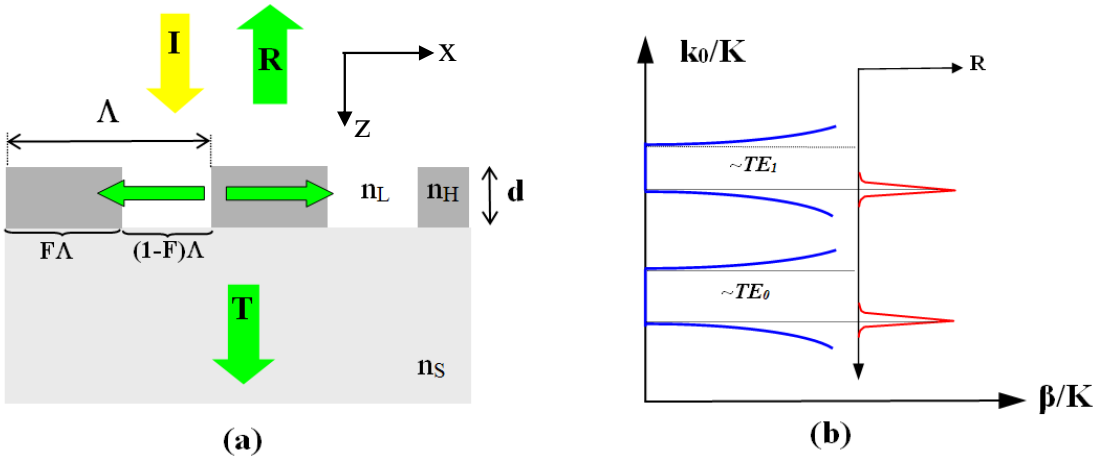

Figure 1. (a) A schematic view of a subwavelength guided-mode resonance lattice element under normal incidence. A single silicon layer with thickness d, fill factor F, and a two-part period Λ is treated. When phase matching occurs between evanescent diffraction orders and a waveguide mode, a reflection resonance takes place. I, R, and T denote the incident wave, reflectance, and transmittance, respectively. (b) Schematic dispersion diagram of a GMR device at the second (leaky) stop band. For the symmetric grating profile, a resonance appears at one edge. This picture applies to both TE (electric field vector normal to the plane of incidence) and TM (magnetic field vector normal to the plane of incidence) polarization states. $K = 2\pi/\Lambda$, $k_0 = 2\pi/\lambda$, and β is the propagation constant of a leaky mode.

The reflector in Fig. 1(a) works under guided-mode resonance (GMR), which arises when the incident wave couples to a leaky Bloch waveguide mode by phase matching with the second-order grating [6,7,10,11]. For normal plane-wave incidence, counter-propagating leaky modes form a standing wave in the grating as indicated in Fig. 1(a). These waveguide modes interact with the grating and reradiate reflectively [11]. We show a schematic dispersion diagram in Fig. 1(b). The device works in the second (leaky) stop band corresponding to the second-order grating [13]. A given evanescent diffraction order can excite not just one but several leaky modes. Thus, in Fig. 1(b), we show the stop bands for the first two TE modes to emphasize this point. At each stop band, a resonance is generated as denoted in Fig. 1(b) also. The fields radiated by these leaky modes in a grating with a symmetric profile can be in phase or out of phase at the edges of the band [1,10]. At one edge, there is a zero phase difference and hence the radiation is enhanced while at the other edge, there is a π phase difference inhibiting the radiation. In this case, if $\beta = \beta_R + j\beta_I$ is the complex propagation constant of the leaky mode, $\beta_I = 0$ at one edge, implying that no leakage is possible at that edge. We remark that the most common variety of resonance elements possesses two-part periods which can only have symmetric profiles.

The bands in Fig. 1(b) exhibit numerous interesting properties. Depending on the device design, the leaky band edge can be placed under or above the band gap. Thus, the fundamental properties of the photonic band structure of resonant leaky-mode metamaterials are of key importance [34,35]. Consistent with the discussion of Fig. 1(b), the band structure admits a leaky edge and a non-leaky edge for each supported resonant Bloch mode if the lattice is symmetric. The non-leaky edge is associated with what is now called a bound state in the continuum (BIC), or embedded eigenvalue, currently of considerable scientific interest [36-39]. It is possible to control the width of the leaky band gap by lattice design. In particular, as a modal band closes, there results a quasi-degenerate state—this state is remarkable as it is possible to transit to it by parametric and material choice. The transition to, and across, this point executes a band flip. The physical mechanisms inducing the band closure and the band flip are of fundamental interest.

Figure 2 illustrates these ideas schematically. As noted in Fig. 2(a), we employ a single 1D periodic layer with thickness d with binary dielectric-constant modulation enclosed by a substrate with dielectric constant ε_s and a cover region of ε_c. The periodic layer acts as a waveguide as well as a phase-matching element because its average dielectric constant $\varepsilon_{avg} = \varepsilon_l + \rho(\varepsilon_h - \varepsilon_l)$ is larger than ε_s and ε_c, where ε_h and ε_l represent the high and low dielectric constants, respectively, and ρ is the fill factor of the high dielectric constant part. The normally incident light is in the TE polarization state such that the electric field vector is along the y-direction. As shown in Fig. 2(b) when the values of ρ and $\Delta\varepsilon=\varepsilon_h - \varepsilon_l$ are small, GMR (BIC in a red circle) occurs at the lower (upper) side of the second stop band. The band flip refers to the transition of the GMR (BIC) location from lower (upper) to upper (lower) band edge as ρ and $\Delta\varepsilon$ increase.

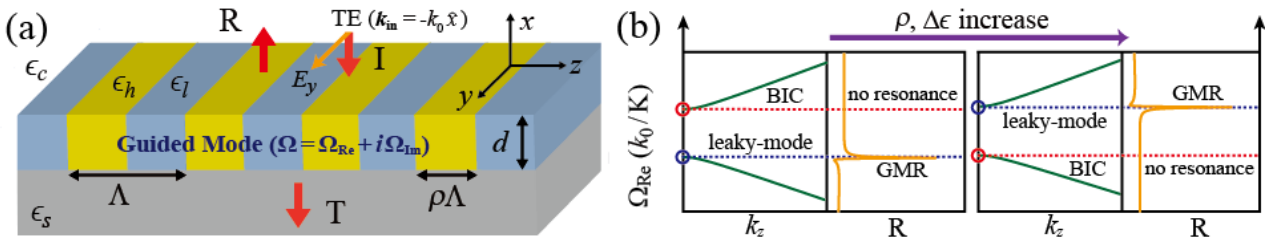

Figure 2. Band flip in a leaky-mode resonant photonic lattice. (a) Schematic of a resonant lattice with a normally-incident TE-polarized plane wave. (b) Conceptual illustration of the band flip phenomenon. When the values of ρ and $\Delta\varepsilon$ are small, GMR (BIC in a red circle) occurs at the lower (upper) side of the second stop band. The band flip denotes the transition of the GMR location from lower to upper band edge as ρ and $\Delta\varepsilon$ increase with the BIC edge transiting oppositely. Here, ρ = F =fill factor, $\Delta\varepsilon = \varepsilon_h - \varepsilon_l$ is the dielectric contrast in the period, and Ω denotes complex frequency. Adapted from reference [35].

It can be shown that the frequency location of the leaky-mode resonance band edge, or the BIC edge, is determined by superposition of Bragg processes denoted by $BR_{Q,n}$ where Q indicates the Bragg order and n denotes the Fourier harmonic of the dielectric constant modulation [35]. Reviewing briefly, as an approximation, we keep only the strongest Bragg processes which are $BR_{2,1}$ operating as a second-order Bragg reflection off the first Fourier harmonic and $BR_{1,2}$ defining a first-order Bragg reflection by the second harmonic. The Bragg reflection superposition model is based on the fact that the size of the second stop band is given by $|\mathrm{Re}(\Omega^+) - \mathrm{Re}(\Omega^-)| = 2|h_2 - \mathrm{Im}(h_1)|/(Kh_3)$ using a semi-analytical model, the

Kazarinov-Henry (KH) model [10], with coupling coefficients h_1 and h_2 related to the first and the second Fourier coefficients, respectively. The band gap will disappear when $h_2=\mathrm{Im}(h_1)$ because the two Bragg reflections $BR_{2,1}$ and $BR_{1,2}$ are then balanced destructively [35]. The veracity of this approach is indicated in Fig. 3.

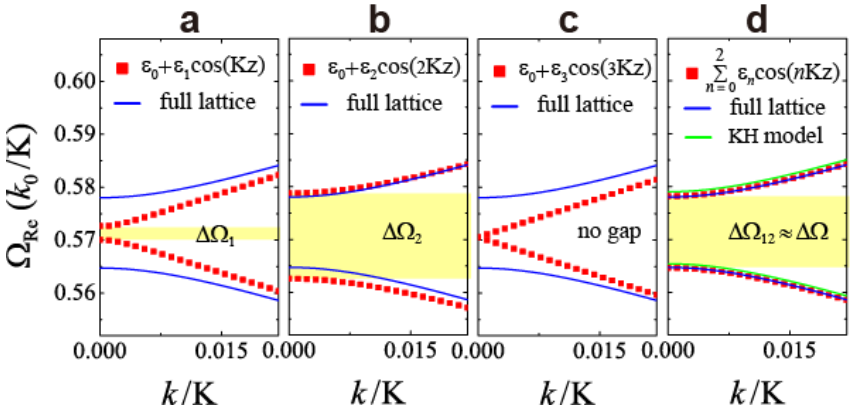

Figure 3. Computed stop bands for a 1D leaky-mode lattice relative to Fourier harmonic content. The dielectric functions vary for these examples. (a) $\varepsilon=\varepsilon_0+\varepsilon_1\cos(Kz)$, (b) $\varepsilon=\varepsilon_0+\varepsilon_2\cos(2Kz)$, and (c) $\varepsilon=\varepsilon_0+\varepsilon_3\cos(3Kz)$. In (d) $\varepsilon=\varepsilon_0+\varepsilon_1\cos(Kz)+\varepsilon_2\cos(2Kz)$ is used. Parameters for the FDTD simulations and KH model are $d=0.50\Lambda$, $\rho=0.35$, $\varepsilon_c=1.00$, $\varepsilon_s=2.25$, $\Delta\varepsilon=1.00$, and $\varepsilon_{avg}=4.00$.

To accurately evaluate stop band formation by these Bragg processes, we calculate the band structures of pertinent 1D lattices by FDTD simulations [35,40]. In Fig. 3(a), for a representative set of lattice parameters provided in the figure caption, the stop band denoted $\Delta\Omega_1$ is shown for a lattice having only the fundamental harmonic $\varepsilon(z)=\varepsilon_0+\varepsilon_1\cos(Kz)$. Dispersion curves (blue lines) obtained from the full non-approximated lattice are also plotted for comparison. Clearly, the FDTD results with the fundamental harmonic only are quite different from those with the full lattice. Figure 3(b) shows stop band $\Delta\Omega_2$ formed by a first-order scattering process off the second harmonic. The full-lattice band structure is close to the approximate structure denoting the importance of this partial scattering process. Figure 3(c) shows that the third order harmonic cannot contribute to the second stop band by itself. Figure 3(d) illustrates that the band $\Delta\Omega_{12}$ simulated with the first and second harmonics simultaneously agrees well with the band $\Delta\Omega$ simulated with the full non-approximated lattice. Moreover, there is excellent agreement with the dispersion curves calculated with the KH model as seen in Fig. 3(d). Hence, it is reasonable to conclude that the Bragg-reflection superposition model presented here is valid to describe the second stop band of weakly to moderately modulated photonic lattices.

3. BLOCH WAVE VECTOR CONTROL OF SPECTRAL CHARACTERISTICS

To illustrate another key aspect of leaky-mode photonic lattices, we provide the results of Fig. 4 showing a device schematic and diffraction spectra. The example architecture studied is similar to that in Fig. 2. We excite the device with a TE-polarized plane wave under normal incidence. What fundamental physical processes are at work to generate this robust single-layer bandpass filter performance including wide low sidebands characteristic of multilayer thin-film filters?

In Fig. 4(b), the high-reflection band shown with $R_0>99\%$ covers 2.165 μm or 20.4%. In this case, the low sidebands are entirely generated by the high-reflectance band. The total electric field distribution at the T_0 peak wavelength of 10.6 μm shown in the inset of Fig. 1(b) indicates that the transmission peak arises from a second-order coupling (q=2) to the TE_0 mode. As clearly revealed by the totally different response (red dotted curve) of an effective-medium homogeneous film, the low-transmission band is attributed to the broadband resonance effect rather than homogeneous thin-film interference. The response is understood by systematically identifying the resonant modes responsible for the flat sidebands by computing the amplitudes of the coupling orders for various wavelengths [41]. To place this in context, we recall that the y-component of the TE-polarized electric field in the grating can be expressed as [42]

$$E_y(x,z)=\sum_q S_q(z)\exp(-i\boldsymbol{\sigma_q}\cdot\boldsymbol{r})$$

where $\boldsymbol{\sigma}_q = \boldsymbol{\rho} - q\mathbf{K}$ with $\boldsymbol{\rho}$ being the wave vector of the refracted input wave, $\mathbf{K}$ is the grating vector with magnitude $K=2\pi/\Lambda$, and $\mathbf{r} = (x,z)$ is the position vector. This is the coupled-wave expression for the internal field where the S_q is the amplitude of the q-th space harmonic in the inhomogeneous plane-wave expansion. We find that TE_2 and TE_1 types of modes under first (q=1) and second (q=2) order coupling are involved in the formation of the flat low-transmission sidebands [41]. Moreover, a TE_0 mode under dominant second-order coupling induces the narrow T_0 peak in this design. In Fig. 4(b), the inset shows a clear TE_0 mode shape (along the z-direction) while the standing wave pattern induced by the counter-propagating Bloch modes at resonance shows periodicity of $\Lambda/2$ due to the q=2 evanescent diffraction order excitation. This coupling configuration expresses the detailed modal properties of the doubly resonant bandpass filters proposed long ago by Ding and Magnusson [43]. There, and in Fig. 4, the sharp transmission channel arises on account of the resonant interference between a low–Q and high-Q leaky Bloch modes. We note that periodic resonance devices operating in this manner exhibiting a resonant transmission peak have lately been associated with EIT or called EIT-like.

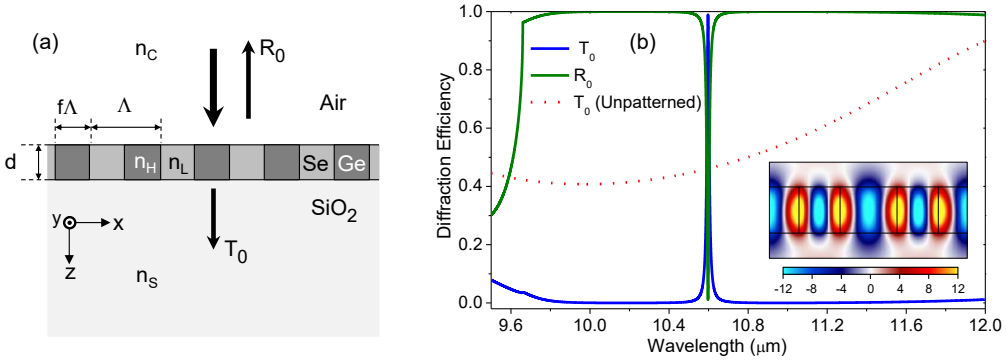

Figure 4. (a) Device schematic and (b) spectral performance of a single-layer GMR bandpass filter with period Λ = 6.91 μm, fill factor f = 0.42, and grating thickness d = 3.8 μm. Refractive indices are n_C = 1 (air), n_S = 1.4 (SiO_2), n_H = 4 (Ge), and n_L = 2.64 (Se). T_0 and R_0 denote the zero-order transmittance and zero-order reflectance, respectively. The dashed line in (b) represents the optical response for the grating layer replaced with the effective homogeneous layer. The inset in (b) shows the distribution of the total electric field over 2Λ at the T_0-peak wavelength. The TE polarization state prevails. After reference [41].

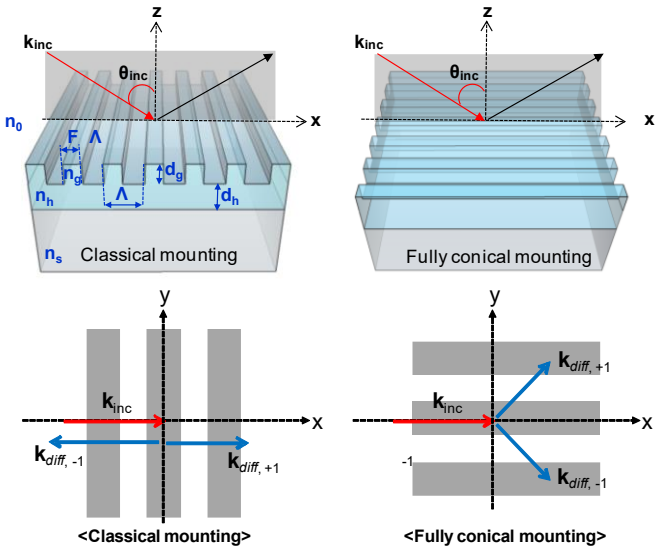

Figure 5. Schematic illustration of 1D subwavelength gratings in classic and fully conic mounts. The grating parameters are grating period (Λ), fill factor (F), grating depth (d_g), and thickness of the homogeneous sublayer (d_h). Here, n_g, n_h, n_s, and n_0 denote the refractive indices of the grating, sublayer, substrate and air. After reference [44].

As another example of Bloch wave vector control, we recall our work on the properties of wideband resonant reflectors under fully conical light incidence. Indeed, the wave vectors pertinent to resonant first-order diffraction under fully conical mounting vary less with incident angle than those for reflectors in classical mounting. Therefore, as the evanescent diffracted waves drive the leaky Bloch modes along their respective wave vectors, fully-conical mounting imbues reflectors with larger angular tolerance than their classical counterparts. This can be understood by Fig. 5. In classical mounting, at normal incidence, the counter-propagating Bloch modes interfere and form a standing wave. As the input angle varies from zero, these modes become imbalanced until one disappears over a possibly small angular range. In contrast, in fully-conic mounting, as the angle deviates from normal, the Bloch-mode wave vectors vary slowly in direction in the lateral plane, neither one vanishing rapidly. This accounts for the angular robustness of wideband reflectors operating in this mounting [44]. Additionally, this methodology has been applied to realize excellent bandpass filters in the laboratory [45].

4. CONCLUSIONS

In conclusion, we present major aspects of leaky-mode photonic lattices explaining key properties with strong reference to flow of lateral Bloch modes. Our lattices are periodic and possess waveguide properties such that quasi-guided modes with finite lifetimes are sustained. The attendant flexible spectral control enables numerous device applications with new attributes relative to prior classic technology. We note that the one-dimensional grating-type canonical model is rich in properties and conceptually transparent encompassing all essential attributes applicable to two-dimensional metasurfaces and periodic photonic slabs. We explain operative physical mechanisms grounded in lateral leaky Bloch mode resonance emphasizing the significant influence imparted by the periodicity and the waveguide characteristics of the lattice. The properties discussed are not explainable in terms of local Fabry-Perot or Mie resonances. Specifically, we summarize the band dynamics of the leaky stopband revealing principal Bragg diffraction processes responsible for band-gap size and band closure conditions. We review Bloch wave-vector influence on spectral characteristics in terms of distinct evanescent diffraction channels driving designated lateral Bloch modes in the lattice. This idea is implemented to configure doubly-resonant bandpass filters as well as to enhance angular robustness in guided-mode resonance spectra. The doubly-resonant bandpass-filter process, actualized by interference between high-Q and low-Q lateral Bloch modes, has been connected with EIT processes in metamaterials in recent literature.

ACKNOWLEDGEMENTS

The research was supported, in part, by the UT System Texas Nanoelectronics Research Superiority Award funded by the State of Texas Emerging Technology Fund as well as by the Texas Instruments Distinguished University Chair in Nanoelectronics endowment. Additional support was provided by the National Science Foundation (NSF) under Awards No. ECCS-1606898 and ECCS-1809143.

REFERENCES

[1] P. Vincent and M. Neviere, “Corrugated dielectric waveguides: a numerical study of the second-order stop bands,” Appl. Phys. 20, 345-351 (1979).
[2] E. Popov, L. Mashev, and D. Maystre, “Theoretical study of the anomalies of coated dielectric gratings,” Optica Acta 33, 607-619 (1986).
[3] I. A. Avrutsky and V. A. Sychugov, “Reflection of a beam of finite size from a corrugated waveguide,” J. Mod. Opt. 36, 1527-1539 (1989).
[4] G. A. Golubenko, A. S. Svakhin, V. A. Sychugov, and A. V. Tishchenko, “Total reflection of light from a corrugated surface of a dielectric waveguide,” Sov. J. Quantum Electron. 15, 886-887 (1985)
[5] H. Kikuta, H. Toyota, and W. Yu, “Optical elements with subwavelength structured surfaces,” Opt. Rev. 10, 63-73 (2003).
[6] S. Wang and R. Magnusson, “Theory and applications of guided-mode resonance filters,” Appl. Opt., 32, 2606-2613 (1993).
[7] Y. Ding and R. Magnusson, “Resonant leaky-mode spectral-band engineering and device applications,” Opt. Express 12, 5661-5674 (2004).

[8] R. Magnusson and S. S. Wang, “New principle for optical filters,” Appl. Phys. Lett. 61(9), 1022-1024 (1992).
[9] W. Suh and S. Fan, “All-pass transmission or flattop reflection filters using a single photonic crystal slab,” Appl. Phys. Lett. 84, 4905-4907 (2004).
[10] R. F. Kazarinov and C. H. Henry, “Second-order distributed feedback lasers with mode selection provided by first-order radiation losses,” IEEE J. Quantum Electron. QE-21, 144-150 (1985).
[11] D. Rosenblatt, A. Sharon, and A. A. Friesem, “Resonant grating waveguide structures,” IEEE J. Quantum Electron. 33, 2038-2059 (1997).
[12] M T. Tamir and S. Zhang, “Resonant scattering by multilayered dielectric gratings,” J. Opt. Soc. Am. A 14, 1607-1616 (1997).
[13] C Y. Ding and R. Magnusson, “Band gaps and leaky-wave effects in resonant photonic-crystal waveguides,” Opt. Express 15, 680-694 (2007).
[14] D. Gerace and L. C. Andreani, “Gap maps and intrinsic diffraction losses in one-dimensional photonic crystal slabs,” Phys. Rev. E 69, 056603 (2004).
[15] S. T. Thurman and G. M. Morris, “Controlling the spectral response in guided-mode resonance filter design,” Appl. Opt. 42, 3225-3223 (2003).
[16] K. J. Lee, R. L. Comb, B. Britton, M. Shokooh-Saremi, H. Silva, E. Donkor, Y. Ding, and R. Magnusson, “Silicon-layer guided-mode resonance polarizer with 40-nm bandwidth,” IEEE Photonics Technol. Lett. 20, 1857-1859 (2008).
[17] R. Magnusson, D. Wawro, S. Zimmerman and Y. Ding, “Resonant photonic biosensors with polarization-based multiparametric discrimination in each channel,” Sensors 11, 1476-1488 (2011).
[18] H. Wu, J. Hou, W. Mo, D. Gao, and Z. Zhou, “A broadband reflector using a multilayered grating structure with multi-subpart profile,” Appl. Phys. B 99, 519–524 (2010).
[19] S. Peng and G. M. Morris, “Resonant scattering from two-dimensional gratings,” J. Opt. Soc. Am. A 13, 993-1005 (1996).
[20] R. Magnusson, “Wideband reflectors with zero-contrast gratings,” Opt. Lett. 39, 4337-4340 (2014).
[21] C. F. R. Mateus, M. C. Y. Huang, Y. Deng, A. R. Neureuther, and C. J. Chang-Hasnain, “Ultrabroadband mirror using low-index cladded subwavelength grating,” IEEE Photon. Technol. Lett. 16, 518–520 (2004).
[22] Mohammad J. Uddin, Tanzina Khaleque, and Robert Magnusson, “Guided-mode resonant polarization-controlled tunable color filters,” Optics Express 22, 12307–12315 (2014).
[23] Kyu J. Lee, James Curzan, Mehrdad Shokooh-Saremi, and Robert Magnusson, “Resonant wideband polarizer with single silicon layer,” Applied Physics Letters 98, 211112-1–211112-3 (2011).
[24] Jae Woong Yoon, Kyu Jin Lee, and Robert Magnusson, “Ultra-sparse dielectric nanowire grids as wideband reflectors and polarizers,” Optics Express 23, 28849-28856 (2015).
[25] Yeong Hwan Ko, Kyu Jin Lee, and Robert Magnusson, “Experimental demonstration of wideband multimodule serial reflectors,” Optics Express 25, 8680-8689 (2017).
[26] Manoj Niraula, Jae Woong Yoon, and Robert Magnusson, “Concurrent spatial and spectral filtering by resonant nanogratings,” Optics Express 23, 23428-23435 (2015).
[27] Manoj Niraula, Jae Woong Yoon, and Robert Magnusson, “Single-layer optical bandpass filter technology,” Optics Letters 40, 5062-5065 (2015).
[28] Robert Magnusson, Debra Wawro, Shelby Zimmerman, and Yiwu Ding, “Resonant Photonic Biosensors with Polarization-based Multiparametric Discrimination in Each Channel,” Sensors: Special Issue Optical Resonant Sensors 11, 1476–1488 (2011).
[29] Yeong Hwan Ko and Robert Magnusson, "Wideband dielectric metamaterial reflectors: Mie scattering or leaky Bloch mode resonance?," Optica 5, 289-294 (2018).
[30] Wang, S. S., Magnusson, R., Bagby, J. S. and Moharam, M. G., “Guided-mode resonances in planar dielectric layer diffraction gratings,” J. Opt. Soc. Am. A 7, 1470-1474 (1990).
[31] Slovick, B., Yu, Z. G., Berding, M. and Krishnamurthy, S. “Perfect dielectric-metamaterial reflector,” Phys. Rev. B 88, 165116 (2013).
[32] Moitra, P., Slovick, B. A., Yu, Z. G., Krishnamurthy, S. and Valentine, J. "Experimental demonstration of a broadband all-dielectric metamaterial perfect reflector", Appl. Phys. Lett. 104, 171102 (2014).
[33] Yu, Y. F., Zhu, A. Y., Paniagua-Domínguez, R., Fu, Y, H., Luk’Yanchuk, B. and Kuznetsov, A. I., “High transmission dielectric metasurface with 2π phase control at visible wavelengths,” Laser Photon. Rev. 9, 412-418 (2015).
[34] Sun-Goo Lee and Robert Magnusson, “Band flips and bound-state transitions in leaky-mode photonic lattices,” arXiv preprint arXiv:1804.02598 (2018).

[35] Sun-Goo Lee and Robert Magnusson, “Band flips and bound-state transitions in leaky-mode photonic lattices,” Phys. Rev. B 99, 045304 (2019).
[36] A. Kodigala, T. Lepetit, Q. Gu, B. Bahari, Y. Fainman, and B. Kanté, “Lasing action from photonic bound states in continuum,” Nature 541, 196–199 (2017).
[37] J. Gomis-Bresco, D. Artigas and L. Torner, “Anisotropy-induced photonic bound states in the continuum,” Nature Photonics 11, 232-236 (2017).
[38] C. W. Hsu, B. Zhen, A. D. Stone, J. D. Joannopoulos, and M. Soljacic, “Bound states in the continuum”, Nature Reviews Materials 1, 1–13 (2016).
[39] D. C.Marinica, A. G. Borisov, and S. V. Shabanov, “Bound states in the continuum in photonics,” Phys. Rev. Lett. 100, 183902 (2008).
[40] A. Taflove, Computational Electrodynamics: The Finite-Difference Time-Domain Method (Artech House, Boston, 1995).
[41] Manoj Niraula, Jae Woong Yoon, and Robert Magnusson, “Mode-coupling mechanisms of resonant transmission filters,” Optics Express 22, 25817-25829 (2014).
[42] T. K. Gaylord and M. G. Moharam, “Analysis and applications of optical diffraction by gratings,” Proc. IEEE 73, 894-937 (1985).
[43] Y. Ding and R. Magnusson, “Doubly resonant single-layer bandpass optical filter,” Opt. Lett. 29, 1135-1137 (2004).
[44] Yeong Hwan Ko, Manoj Niraula, Kyu Jin Lee, and Robert Magnusson, “Properties of wideband resonant reflectors under fully conical light incidence,” Opt. Express 24, 4542-4551 (2016).
[45] Manoj Niraula, Jae Woong Yoon, and Robert Magnusson, “Single-layer optical bandpass filter technology,” Opt. Lett. 40, 5062-5065 (2015).